

1 **Contact tracing efficiency, transmission heterogeneity, and accelerating COVID-**
2 **19 epidemics**

3

4 Billy J. Gardner, A. Marm Kilpatrick*

5

6 *Department of Ecology and Evolutionary Biology, University of California, Santa Cruz*

7 **Correspondence to akilpatr@ucsc.edu*

8

9

10 **Abstract**

11 Simultaneously controlling COVID-19 epidemics and limiting economic and societal
12 impacts presents a difficult challenge, especially with limited public health budgets.
13 Testing, contact tracing, and isolating/quarantining is a key strategy that has been used
14 to reduce transmission of SARS-CoV-2, the virus that causes COVID-19. However,
15 manual contact tracing is a time-consuming process and as case numbers increase it
16 takes longer to reach each cases' contacts, leading to additional virus spread. Delays
17 between symptom onset and being tested (and receiving results), and a low fraction of
18 symptomatic cases being tested and traced can also reduce the impact of contact
19 tracing on transmission. We examined the relationship between cases and delays and
20 the pathogen reproductive number R_t , and the implications for infection dynamics using
21 a stochastic compartment model of SARS-CoV-2. We found that R_t increases
22 sigmoidally with the number of cases due to decreasing contact tracing efficacy. This
23 relationship results in accelerating epidemics because R_t increases, rather than
24 declines, as infections increase. Shifting contact tracers from locations with high and
25 low case burdens relative to capacity to locations with intermediate case burdens
26 maximizes their impact in reducing R_t (but minimizing total infections is more
27 complicated). Contact tracing efficacy also decreased with increasing delays between
28 symptom onset and tracing and with lower fraction of symptomatic infections being
29 tested. Finally, testing and tracing reductions in R_t can sometimes greatly delay
30 epidemics due to the highly heterogeneous transmission dynamics of SARS-CoV-2.
31 These results demonstrate the importance of having an expandable or mobile team of
32 contact tracers that can be used to control surges in cases, and the value of easy
33 access, high testing capacity and rapid turn-around of testing results, as well as
34 outreach efforts to encourage symptomatic infections to be tested immediately after
35 symptom onset.

36

37 **Author Summary**

38 A key tool in the control of infectious diseases is contact tracing – the
39 identification of individuals who have contacted the case and may have been infected
40 by a newly detected case. However, to successfully contact and quarantine individuals
41 requires time, and as cases rise, this can result in delays in reaching contacts during
42 which time they may infect other people. Here we examine the quantitative relationships
43 between increasing case numbers, contact tracing efficiency, and the pathogen
44 reproductive number R_t (the number of cases infected by each case) and how these
45 relationships vary with delays and incomplete participation in the testing and tracing
46 process. We built

47

48 **Introduction**

49 Severe acute respiratory syndrome coronavirus 2 (SARS-CoV-2) emerged in late
50 2019 spread globally in early 2020 and resulted in rapidly growing local epidemics, large
51 scale mortality, and strains on hospital capacity in many countries (1-4). Initial outbreaks
52 in most countries and US states were arrested only by severe control measures
53 including closing all but essential businesses as well as schools, churches, and other
54 organizations (5), while a few countries were able to limit transmission, at least
55 temporarily, primarily with public health measures (6-8). Severe disease control
56 measures have had devastating impacts on economies and societies (5). Most
57 countries and US states are now attempting to re-open as many business sectors and
58 activities as possible while avoiding a rapid rise in infections.

59 Although self-isolation, social distancing, and mask wearing have reduced the
60 transmission of SARS-CoV-2, additional interventions, including business closures and
61 working from home, have often been required to keep the pathogen reproductive
62 number R_t below 1 (5, 9, 10), especially in the United States. One public health strategy
63 that has been used effectively to limit transmission in some countries is testing
64 symptomatic individuals, tracing their contacts to people they may have infected, and
65 isolating infected individuals and quarantining people that may have become infected
66 but have yet to show symptoms or test positive for the virus (hereafter abbreviated T-

67 CT-I/Q) (7, 10, 11). If contacts of cases can be found and quarantined or isolated before
68 or during their infectious period, this can limit onward spread of the virus.

69 Numerous studies have examined the effectiveness and limitations of T-CT-I/Q
70 on transmission of SARS-CoV-2 (11-18). Many studies have shown that T-CT-I/Q can
71 substantially reduce the pathogen reproductive ratio, R_t , but its efficacy depends on the
72 importance of pre-symptomatic and asymptomatic transmission, delays between
73 symptom onset and being tested, and the fraction of infections that are tested and
74 traced (11, 15, 18). Previous studies have explored various parameter values for
75 contact tracing efficacy by varying the fraction isolated, the fraction symptomatic, and
76 the contribution to transmission of undetected infections (11, 15, 18). A key unexplored
77 challenge in implementing T-CT-I/Q is that tracing contacts and ensuring they can
78 safely quarantine or isolate is a time-consuming process which results in delays
79 between detecting a case and successfully quarantining their contacts. This delay
80 reduces the effectiveness of contact tracing as cases increase. Previous studies have
81 assumed fixed values for contact tracing parameters and thus have not addressed this
82 issue.

83 Our aim was to examine the relationship between increasing cases, contact
84 tracing efficacy, and the pathogen reproductive ratio, R_t , and to examine the potential
85 outcomes for disease dynamics. We built a compartment model of SARS-CoV-2
86 transmission, parameterized it with data from the literature, and examined how R_t varied
87 with number cases traced, delays between symptom onset and the start of contact
88 tracing, the numbers of contacts per case, and different fractions of symptomatic cases
89 being tested and traced. We also simulated a stochastic version of the model with and
90 without contact tracing to examine how reductions in R_t affected variation in the timing
91 of epidemics.

92

93 **Methods**

94 We built a susceptible-exposed-infected-recovered (SEIR) compartment model of
95 SARS-CoV-2 that included four compartments for infected individuals that reflect
96 symptom severity (asymptomatic, I_a , pre-symptomatic, I_{ps} , mildly symptomatic, I_{ms} , and
97 severely symptomatic, I_{ss}) (Fig S1). The equations of the model are:

98

$$99 \quad dS/dt = -\kappa\beta S/N(\sigma_a I_a + \sigma_{ps} I_{ps} + \sigma_{ms} I_{ms} + \sigma_{ss} I_{ss})$$

$$100 \quad dE/dt = \kappa\beta S/N(\sigma_a I_a + \sigma_{ps} I_{ps} + \sigma_{ms} I_{ms} + \sigma_{ss} I_{ss}) - (\varepsilon + q_{E \rightarrow ps} + q_{E \rightarrow a}) E$$

$$101 \quad dI_{ps}/dt = q_{E \rightarrow ps} E - (\varepsilon + q_{ps \rightarrow ms}) I_{ps}$$

$$102 \quad dI_a/dt = q_{E \rightarrow a} E - (\varepsilon + \gamma_a) I_a$$

$$103 \quad dI_{ms}/dt = q_{ps \rightarrow ms} I_{ps} - (\varepsilon + \tau_{ms} + q_{ms \rightarrow ss} + \gamma_{ms}) I_{ms} \quad [\text{eq. 1}]$$

$$104 \quad dI_{ss}/dt = q_{ms \rightarrow ss} I_{ms} - (\varepsilon + \tau_{ss} + \alpha + \gamma_{ss}) I_{ss}$$

$$105 \quad dQ/dt = \varepsilon I_a + \varepsilon I_{ps} + (\varepsilon + \tau_{ms}) I_{ms} + (\varepsilon + \tau_{ss}) I_{ss} - \gamma_Q Q$$

$$106 \quad dR/dt = \gamma_a I_a + \gamma_{ms} I_{ms} + \gamma_{ss} I_{ss} + \gamma_Q Q$$

107

108 where κ is a social distancing factor between 0 and 1 that scales the contact rate β , σ
 109 are relative infectiousness values for each of the I classes, q are transition rates
 110 between classes given by the subscripts separated by the arrow ($q_{E \rightarrow ps}$ is the transition
 111 rate between the E and I_{ps} classes), ε is the rate of removal by contact tracing from the
 112 E or I classes to the quarantined class Q, τ are the removal rate by testing of mildly
 113 symptomatic or severely symptomatic infected individuals, α is the disease-caused
 114 death rate, and γ are the recovery rates to the R class.

115 The contact tracing removal rate ε is given by:

$$116 \quad \varepsilon = \frac{f_{SCT} q_{E \rightarrow ps}}{q_{E \rightarrow ps} + q_{E \rightarrow a}} \frac{1}{1/\tau_{ms} + 0.5 \frac{I_{ps} q_{ps \rightarrow ms} N_{CPC}}{N_{CT} N_{CCTD}}} \quad [\text{eq. 2}]$$

117 The first term is the fraction of infections traced; f_{SCT} is the fraction of symptomatic
 118 infections that are traced of those detected with test removal rate τ_{ms} before they
 119 recover or progress to severe symptoms; f_{SCT} is equal to $f_{tmstr} * \tau_{ms} / (\tau_{ms} + q_{ms \rightarrow ss} + \gamma_{ms})$; f_{SCT}
 120 is multiplied by the ratio of transition rates [$q_{E \rightarrow ps} / (q_{E \rightarrow ps} + q_{E \rightarrow a})$] which is the fraction of
 121 infections that are symptomatic; f_{tmstr} is the fraction of mildly symptomatic cases
 122 detected by testing that were traced. We didn't include tracing from severely
 123 symptomatic cases because, by the time an infection progresses to severe symptoms
 124 5-8 days after symptom onset (19, 20), their contacts will already have finished most of
 125 their infectious period, and quarantining their contacts will have little effect.

126 The second term is the inverse of the time between symptom onset of the

127 symptomatic infection and being removed by contact tracing which is the sum of the
128 delay between symptom onset and receiving a test result, $1/\tau_{ms}$, and the average time
129 needed to reach the contacts of the newly detected cases (which is half the total time to
130 call all contacts). $q_{ps \rightarrow ms} I_{ps}$ is the rate of new symptomatic infections that need to be
131 traced, N_{cpc} is the average number of contacts per case, N_{CT} is the number of contact
132 tracers, and N_{CCTD} is the number of calls each contact tracer can make each day.

133 We parameterized the model with data from the literature, with all rates in days⁻¹
134 (Table 1) and used the baseline contact tracing capacity standards suggested by the
135 US National Association of County and City Health Officials (15 contact tracers per
136 100,000 people; <https://www.naccho.org/uploads/full-width-images/Contact-Tracing-Statement-4-16-2020.pdf>). We note that while notifying individuals that they have had
138 contact with a case can be done quickly (especially with using a cell-phone tracing app;
139 (18)), successfully ensuring a contact has their needs met (including food, medicine,
140 clothing) to quarantine in a safe space where they won't infect their household members
141 requires substantially more time (<https://www.cdc.gov/coronavirus/2019-ncov/php/notification-of-exposure.html>). We assumed the approximate duration required
142 for a successful contact tracing call was 40 min, resulting in $N_{CCTD} = 12$

144 We used the next generation matrix technique to derive an expression for the
145 pathogen reproductive ratio R_t (21):

146

147 $R_t = S/N[\kappa\beta]^*$

148
$$[[(q_{E \rightarrow a})(\sigma_a) / (\epsilon + \gamma_a)] + [(q_{E \rightarrow ps})(\sigma_{ps}) / (\epsilon + q_{ps \rightarrow ms})] + \quad [eq. 3]$$

149
$$[(q_{E \rightarrow ps})(q_{ps \rightarrow ms})(\sigma_{ms}) / ((\epsilon + q_{ps \rightarrow ms})(\epsilon + \tau_{ms} + q_{ms \rightarrow ss} + \gamma_{ms}))] +$$

150
$$[(q_{E \rightarrow ps})(q_{ps \rightarrow ms})(q_{ms \rightarrow ss})(\sigma_{ss}) /$$

151
$$((\epsilon + q_{ps \rightarrow ms})(\epsilon + \tau_{ms} + q_{ms \rightarrow ss} + \gamma_{ms})(\epsilon + \tau_{ss} + \alpha + \gamma_{ss}))]] / (\epsilon + q_{E \rightarrow a} + q_{E \rightarrow ps})$$

152

153 This expression can be understood as the fraction of the population that is susceptible,
154 S/N multiplied by the contact rate β (which is scaled by the social distancing factor κ),
155 multiplied by the sum of four terms: one for each infected class. Each of the four terms
156 includes the product of the transition rates q to reach that class from the E class
157 multiplied by the infectiousness of that class, σ , divided by the recovery, testing and

158 tracing rates leaving that I class and the I classes before it. Finally, all four terms are
159 divided by the rates hosts leave the E class which normalizes the rates moving along
160 each infection pathway.

161 We examined how R_t and R_0 ($R_t = R_0$ at beginning of epidemic when $S \cong N$)
162 varied with different numbers of new symptomatic cases detected (a fraction of the
163 newly symptomatic infection, $I_{ps} q_{ps \rightarrow ms}$ in eq. 2), delays between symptom onset and the
164 start of contact tracing ($1/\tau_{ms}$ in eq. 2), and numbers of contacts per case (N_{cpc} in eq. 2).
165 Note that because these three quantities occur as a ratio (with the number of contact
166 tracers) in equation (2), any combination of values that produce the same number of
167 case-contacts per contact tracer calls per day will produce the same value of R_t . We
168 illustrated the effect of decreasing contact tracing efficiency as infections increased on
169 disease dynamics and R_t by simulating a deterministic version of the model in eq. 1 and
170 plotted R_t in real time as an epidemic swept through a population over one year. We
171 also performed a simple sensitivity analysis by determining how much R_t varied with a
172 ten percent increase or decrease in each model parameter (Fig S2).

173 Finally, we explored the implications of stochastic variability and contact tracing
174 on infection dynamics in a scenario roughly based on a moderate size city with partly
175 effective social distancing. We simulated a stochastic version of the model given by eq
176 1 where the number of new infections was drawn from a negative binomial distribution
177 with mean equal to R_t and dispersion parameter 0.16 which is intermediate between
178 available estimates for COVID-19 (22-24). We modeled a scenario of a population of
179 100,000 people where non-pharmaceutical interventions reduced contact rates by 30%
180 ($\kappa=0.7$) resulting in R_0 with/without contact tracing of 1.32/1.67, testing and contact
181 tracing took place after an average of $1/\tau_{ms} = 5$ days after symptom onset, and half of
182 symptomatic cases detected by testing being traced ($f_{tmstr} = 0.5$). We examined different
183 initial numbers of latently infected individuals, E , at the start of the epidemic to
184 understand how stochastic variation could impact the timing of epidemics when initial
185 infections were low.

186 R code to reproduce the results is available from:
187 <https://github.com/marmkilpatrick/Contact-Tracing-Efficiency>

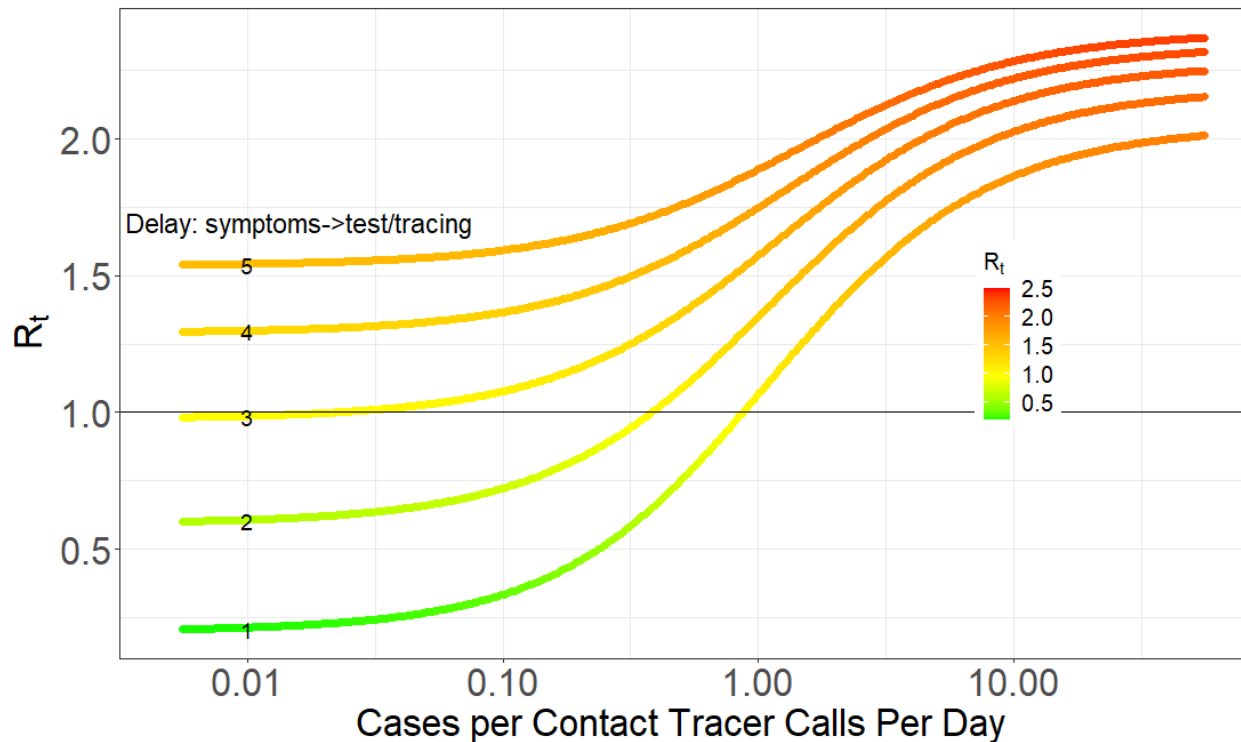
188

189

190 Results

191 The effectiveness of contact tracing in reducing the pathogen reproductive
192 number, R_t , was highly dependent on three factors: the number of cases being traced
193 (given a fixed number of contact tracers), the delay between symptom onset and the
194 start of tracing, $1/\tau_{ms}$, (including getting tested and receiving result), and the fraction of
195 symptomatic cases that get traced (Figs 1-3).

196

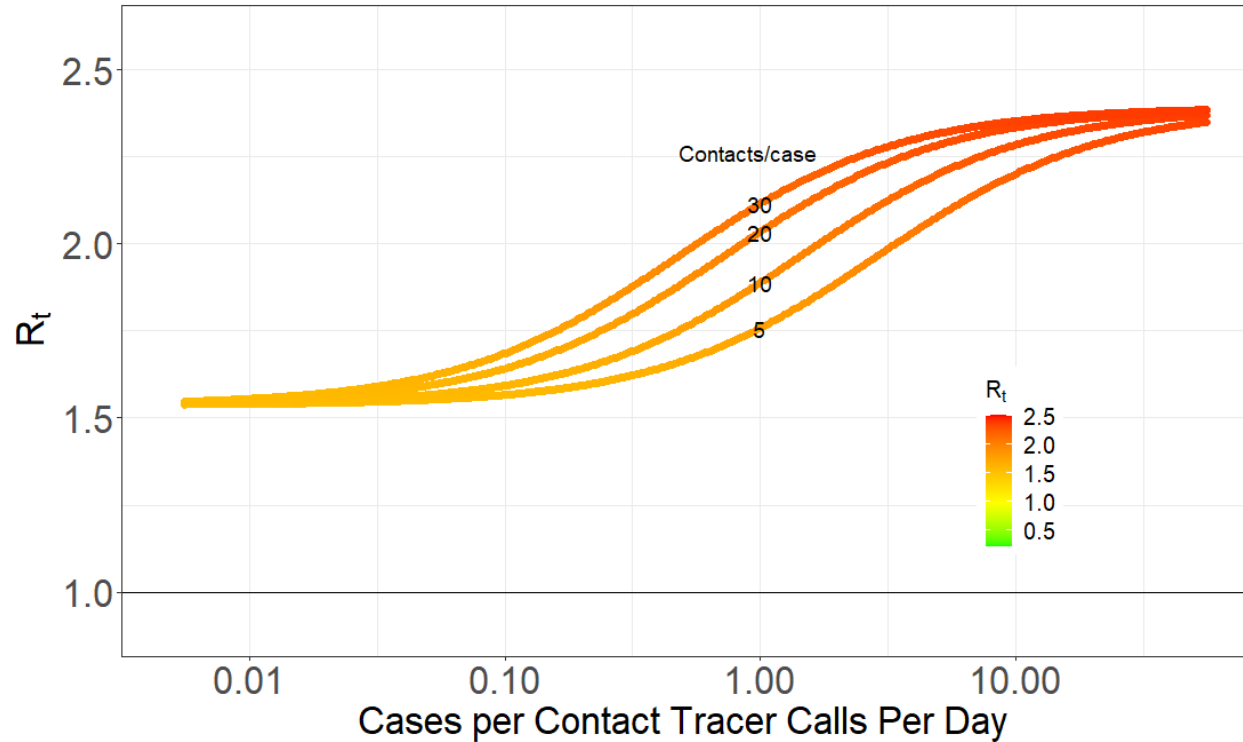


197

198 **Figure 1. Pathogen reproductive ratio R_t plotted against the number of new cases**
199 **per contact tracer calls per day for 1-5 day delays ($1/\tau_{ms}$) between symptom onset**
200 **and the start of contact tracing (including getting tested and receiving result), 10**
201 **contacts per case (so the average number of contacts each tracer has to reach**
202 **each day is 10x the x-axis values). With no contact tracing R_t increases from 2.03**
203 **to 2.37 as the delay $1/\tau_{ms}$ increases from 1 to 5 days, which is evident in the y-axis**
204 **difference between curves in the upper right of the graph where new case**
205 **burdens are so high contact tracing is ineffective. Delays are indicated by the**
206 **small numbers on each curve in the left of the plot.**

207
208
209
210
211
212
213
214
215
216
217
218
219
220
221
222
223
224

First, the relationship between R_0 and the number of cases per contact tracer calls per day was sigmoid (Figs 1-3); at both high and low numbers adding or removing contact tracers had smaller effects whereas at intermediate case numbers relative to capacity shifting contact tracers would have a larger impact. When the number of new daily cases per contact tracer call per day was high (i.e. >1 or 10 contacts per contact tracer calls per day), contact tracing had relatively little effect in reducing R_0 no matter how long the delay was between symptom onset and the start of tracing, $1/\tau_{ms}$ (right side of Figs 1; also evident in Figs 2, 3). This is because contact tracing calls took too long, on average (>10 days), to reduce the infectious period of contacts. Note that for the parameter estimates used (Table 1), an average case becomes infectious starting 3.2 days after infection, and is highly or moderately infectious for an average of 7.3 more days (σ_{ps} and σ_{ms} ; Table 1). The exponentially distributed durations for the latent and infectious periods implied by standard compartmental models result in only 37% of individuals leaving each class after the average duration, which results in a relatively smaller benefit of contact tracing beyond this case burden, and resultant delay in reaching contacts of cases.



225
226 **Figure 2. Pathogen reproductive ratio R_t plotted against the number of Cases per**
227 **contact tracer calls per day for four different number of contacts per case (5, 10,**
228 **20, 30; indicated by the small numbers on each curve in the middle of the plot),**
229 **and an average delay $1/\tau_{ms}$ of 5 days between symptom onset and contact tracing**
230 **(including getting tested and receiving result). With no contact tracing $R_t = 2.39$.**

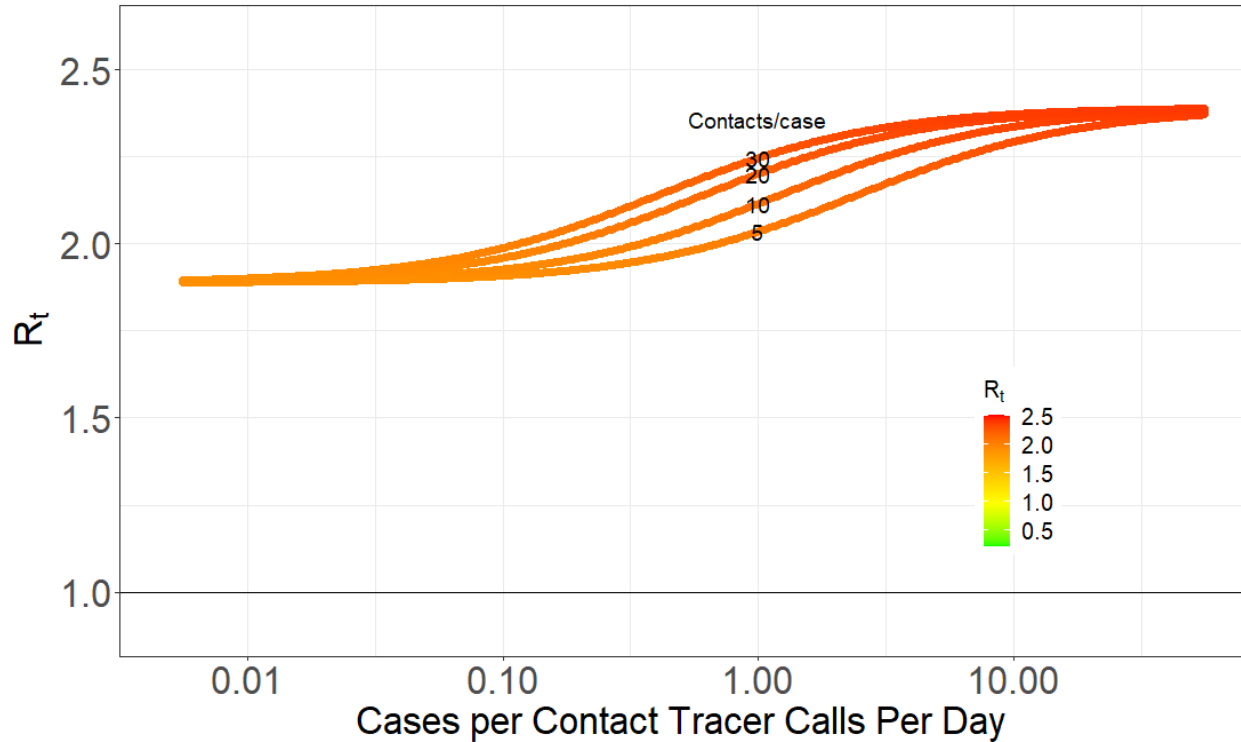
231
232 Contact tracers in regions with very high new case numbers relative to contact
233 tracing capacity (>1 on Fig. 1) would have a larger reduction on R_t if they were tracing
234 calls with intermediate numbers of cases (0.02 to 1 cases/contact tracer calls per day).
235 However, it is worth noting that reducing R_t is not the same as preventing new cases
236 (see Discussion below). Nonetheless, if the goal is to reduce $R_t < 1$ to stop the growth in
237 cases, the analyses in Figs 1-3 suggest that when new case burdens are high relative
238 to capacity, population-wide interventions (e.g. social distancing or different levels of
239 shelter-in-place orders which reduce contact rates, β or κ , and shift the entire curves in
240 Fig 1-3 downward proportionately; Fig. S2), or orders of magnitude increases in contact
241 tracing capacity will be needed until R_t can be effectively reduced by contact tracing.

242 When there are few ($< \sim 0.02$) cases per contact tracer call per day, contact

243 tracing was as effective as it could be but excess capacity had little impact, especially
244 for realistic delays, $1/\tau_{ms}$, between symptom onset and the start of tracing (e.g. 3-5
245 days). Shifting contact tracers to other areas with more cases per contact tracer (0.02 to
246 0.2) would have minimal impact in increasing R_t but could help substantially reduce R_t in
247 those places with higher new case burdens relative to capacity.

248 Second, increasing delays, $1/\tau_{ms}$, between symptom onset and the start of
249 tracing greatly influenced the efficacy of contact tracing (Fig. 1). With a 5 day delay,
250 contact tracing could only reduce R_0 by 33% from 2.6 to 1.6 regardless of contact
251 tracing capacity per case. In contrast, if all symptomatic people sought care and got
252 tested within 1 day of after symptom onset and results were returned within the next 24
253 hours ($1/\tau_{ms} = 2$ days), contact tracing could reduce R_0 by 73% from 2.2 to 0.6. Note
254 that the effect of delays in increasing R_0 due to delayed removal by testing alone (τ_{ms}) is
255 small compared to the effect of delays in reducing contact tracing efficiency (Fig 1:
256 compare differences among curves in upper right of graph where contact tracing is
257 having little effect to differences among curves in lower left of graph where it has
258 maximal effect). The number of contacts per case obviously also influences the time
259 required to trace these contacts (Fig. 2). If allowable (or illegal) gathering sizes
260 increase, this leads to more contacts per case and a faster decrease in contact tracing
261 efficacy.

262 Thirdly, if contacts for a substantial fraction of all symptomatic cases do not get
263 traced and quarantined, T-CT-I/Q is far less effective. Figures 1 and 2 showed an
264 optimistic scenario where the fraction of symptomatic infections that are tested and
265 traced is determined only by the delay between symptom onset and testing results
266 being returned ($1/\tau_{ms}$) (i.e. all symptomatic infections could be tested and traced). With a
267 5 day delay ($1/\tau_{ms}=5$) (Fig. 2), this results in 38% of infections being detected by testing
268 in the mildly symptomatic state (I_{ms}) which is much higher than estimates of case under-
269 ascertainment based on seroprevalence studies (25). If only half of these cases are
270 contact traced ($f_{tmstr} = 0.5$) the maximum impact of contact tracing is smaller: a 21%
271 reduction in R_0 from 2.39 to 1.89 (Fig 3) rather than a 35% decrease from 2.38 to 1.54
272 (Fig 2).



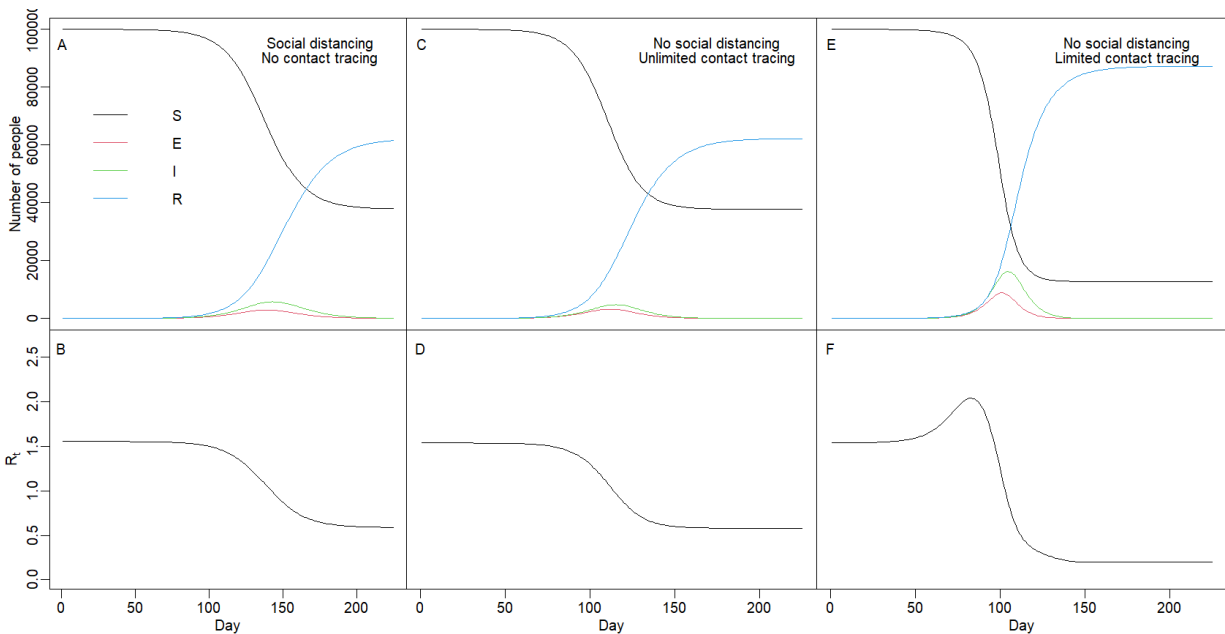
273

274 **Figure 3. Pathogen reproductive ratio R_t plotted against the number of Cases per**
275 **contact tracer calls per day for four different number of contacts per case (5, 10,**
276 **20, 30; indicated by the small numbers on each curve in the middle of the plot), 12**
277 **calls per contact tracer per day, an average delay $1/\tau_{ms}$ of 5 days between**
278 **symptom onset and contact tracing (including getting tested and receiving**
279 **result). This Figure is the same Figure 2, except only half as many contacts are**
280 **traced ($f_{tmstr} = 0.5$). With no contact tracing, $R_t = 2.39$.**

281

282 Reduced contact tracing efficiency with increasing cases can result in a transient
283 accelerating epidemic where R_t increases over time (Fig 4). If contact tracing capacity is
284 insufficient to quickly trace contacts, then a decrease in contact tracing efficiency can
285 initially outweigh the depletion of susceptible individuals and lead to an increase in R_t
286 over time until depletion of susceptibles overwhelms this effect (Fig 4: compare
287 rightmost panels with limited contact tracing to leftmost panels where social distancing
288 reduces R_t to the same initial value as contact tracing). With unlimited contact tracing
289 this phenomenon does not arise (Fig 4: compare middle panels with unlimited contact
290 tracing to leftmost panels).

291



292

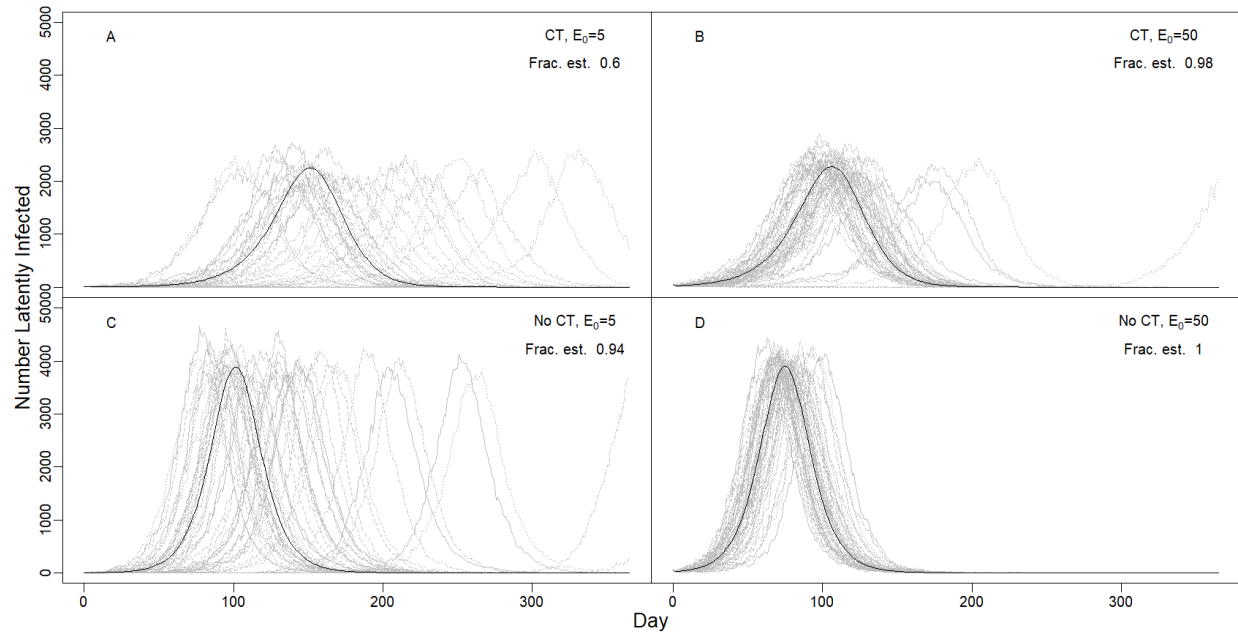
293 **Figure 4. Impact of reduced contact tracing efficiency with increasing cases. Left**
294 **panels show (A) the number of susceptible, exposed, infected, and recovered**
295 **individuals and (B) reproductive number, R_t , over time with no contact tracing but**
296 **social distancing ($\kappa = 0.65$) set to give same initial R_0 (1.55) as with contact**
297 **tracing. Middle panels (C, D) show the same variables with unlimited contact**
298 **tracing (1500 contact tracers making 12 calls/day; 15 contacts per case; $1/\tau_{ms} =$**
299 **5d; $f_{tmstr} = 1$) but no social distancing ($\kappa = 1$). Right panels (E, F) show the same**
300 **variables and parameters as (C, D) but with limited contact tracing (5 contact**
301 **tracers).**

302

303 The impact of contact tracing in reducing the pathogen reproductive number R_t
304 has two consequences on the temporal timing and establishment of epidemics. First, as
305 is well known, reducing R_t delays and reduces the peak of the epidemic (Fig 5 top vs
306 bottom panels). Second, and less appreciated, stochastic variation in R_t can lead to very
307 different timing of epidemics if the initial number of infected individuals is low (Fig 5 left
308 panels), and variation is larger if R_t is lower (Fig 5A vs Fig 5C). Finally, heterogeneity in
309 individual transmission can result in local fadeout of the pathogen and this is more if
310 contact tracing reduces R_t so that it is closer to 1, and if the number of infected

311 individuals is lower.

312



313

314 **Figure 5. Variability in the timing and outcome of epidemics due to stochastic**
315 **variation in individual R_t . Lines show number of latently infected individuals (in**
316 **the E class) over time for 1 year with moderate social distancing that reduces**
317 **contact rates by 30% ($\kappa = 0.7$). Grey lines show a single stochastic simulation and**
318 **the black line shows the deterministic outcome. Frac. est. is the fraction of**
319 **epidemics that establish (i.e. the maximum number of infected at any time**
320 **exceeds the starting number infected). Four scenarios include different starting**
321 **numbers of latently infected individuals on day 0, E_0 (A, C: 5; B, D: 50), and with**
322 **(A, B) or without (C, D) contact tracing (CT) which lowered R_0 from 1.67 to 1.32.**
323 **The delay from symptom onset to testing and tracing was 5d, but only half of**
324 **cases were traced ($f_{tmstr} = 0.5$), as in Fig 3. The modeled population of 100,000**
325 **people had 15 tracers making 12 calls/day, and each case had an average of 15**
326 **contacts which is intermediate between pre-lockdown and lockdown conditions.**

327

328

329 Discussion

330

The two main strategies that have been used to control COVID-19 are T-CT-I/Q

331 and society-wide social distancing interventions (including closing businesses, banning
332 gatherings, wearing masks, etc.) (9). Closing businesses has had devastating impacts
333 on employment and economies, as well as cascading impacts on society. T-CT-I/Q has
334 far smaller economic and societal costs, but its efficacy in controlling epidemics is not
335 fully understood, and some studies suggest that it is insufficient to keep R_t below 1 in
336 many settings, especially without digital contact tracing (10, 11, 18). We examined how
337 the efficacy of contact tracing decreases with increasing case burden. At high case
338 burdens relative to contact tracing capacity, contact tracing reached most contacts too
339 late and had little effect on R_t . Conversely when case numbers were very low relative to
340 contact tracing capacity, there was excess capacity and, all else being equal, contact
341 tracers could be used more effectively in higher case burden settings with very small
342 impacts on local transmission. We note that the exact number of contact tracers needed
343 to reduce R_t depends on the number of contacts per case and the number of calls each
344 tracer can make each day (Fig 2). However, the key quantity appears as a ratio of case-
345 contacts per contact tracer calls per day. Thus, each contact tracing team (e.g. a US
346 County) can use local estimates of contacts per case and the number of calls each
347 tracer can make each day to determine where they are on the modelled relationships
348 (Figs 1-3).

349 A major caveat must be kept in mind in interpreting these results. A smaller
350 reduction in R_t (e.g. 10%) in one population can prevent more infections (especially over
351 multiple generations of transmission) than a larger (e.g. 20%) reduction in R_t in a
352 second population if R_t in the second location is lower (especially when $R_t > 1$ in the first
353 population), or when there is a larger number of infected individuals in the first
354 population. Thus, transferring contact tracers from a region with a high case burden
355 relative to contact tracing capacity to maximize their efficacy in reducing R_t should only
356 be done if other measures (e.g. social distancing) will be put into place to reduce R_t
357 where case numbers are high. More generally, allocation of contact tracers to maximize
358 the number of cases prevented given an array of tools would require a complex
359 dynamic analysis beyond that examined here.

360 We also found that the efficacy of contact tracing itself, regardless of capacity,
361 was strongly influenced by delays between the onset of symptoms and the beginning of

362 tracing, as well as the fraction of symptomatic infections that were traced. Unless delays
363 were short and the fraction of symptomatic cases that were traced was high, contact
364 tracing had limited effects in reducing R_t . This finding parallels results from other studies
365 demonstrating the large effects of delays in reducing efficacy of isolating infections by
366 testing alone (26). We note that in the model considered here, only symptomatic
367 individuals were removed by testing (pre-symptomatic and asymptomatic infections
368 were not tested) which leads to a much smaller impact of testing on R_t . Our results
369 emphasize the importance of encouraging people to get tested as soon as possible
370 after mild symptom onset, and having sufficient testing capacity to return their results
371 quickly. Similarly, the fraction of symptomatic infections that get tested and traced is
372 poorly known, but if the ratio of infections to cases from seroprevalence studies in some
373 locations is approximately correct (e.g. 10:1; (25)), then contact tracing will have very
374 limited effects in reducing transmission.

375 Allocation of contact tracing resources can be most efficiently deployed in two
376 ways. First, contact tracing is much more effective when infections are detected soon
377 after symptom onset. One should prioritize these individual cases for tracing since their
378 contacts are likely to be earlier in their infections and quarantining them will cut off most
379 or all of their infectious period. If one knows the date of contact between the case and
380 the contact, one could also prioritize tracing more recent contacts and those that had
381 contact with the case during the case's days of peak infectiousness just before and after
382 symptom onset (27, 28). Second, if one is attempting to limit transmission in multiple
383 regions (e.g. US counties within a state) one could deploy contact tracers to counties
384 where they will be able to have the most impact: from places with excess capacity to
385 those with intermediate numbers of cases per contact tracer calls per day. Conversely,
386 if contact tracers cannot quarantine the contacts of cases within 10-12 days of the
387 case's symptom onset, they will be unlikely to effectively reduce transmission from
388 those contacts.

389 Our results also offer insight on two phenomena observed in COVID-19
390 epidemics that are not fully understood. First, epidemic dynamics sometimes differ
391 enormously between places that seem otherwise similar. This may be due to
392 differences in social behavior or contact patterns, but our results illustrate that

393 stochastic chance may also play a role in shifting the timing of epidemics by more than
394 a month, especially when the initial number of cases is low and R_t is closer to 1 (i.e.
395 when lockdowns are first lifted) so that populations spend longer periods of time with
396 few cases where stochastic variation is most important. Second, staged business re-
397 openings have sometimes led to accelerating or runaway epidemics. These may be due
398 to sudden changes in social behavior, but decreases in contact tracing efficiency may
399 also contribute to these accelerating epidemics, if contact tracing was playing a
400 significant role in limiting transmission. Increasing contact tracing capacity could limit
401 this epidemic acceleration as cases increase, which suggests that training a reserve
402 capacity of tracers to be used following case surges or being able to deploy a mobile
403 tracing force could help limit runaway epidemics.

404 More broadly, contact tracing could play an important role in limiting transmission
405 of SARS-CoV-2 and other pathogens. However, we found that its efficacy depends on
406 participation in seeking testing immediately following symptom onset and quick return of
407 test results, as well as sufficient contact tracing capacity if case numbers surge.
408 Shortcomings in each of these factors greatly limit its efficacy, which could lead to
409 implementation of much more damaging measures to control transmission, including
410 widespread business and school closures. Investments in public health, including
411 testing, contact tracing, and public outreach to encourage health seeking when
412 symptomatic, is likely a much more cost-effective approach to control COVID-19.

413

414 **Acknowledgements:** We thank the dozens of scientists and public health practitioners
415 who have informed this work through comments and discussions.

416

417 **Literature Cited**

- 418 1. J. T. Wu, K. Leung, G. M. Leung, Nowcasting and forecasting the potential domestic and
419 international spread of the 2019-nCoV outbreak originating in Wuhan, China: a
420 modelling study. *Lancet* **395**, 689-697 (2020).
- 421 2. A. Remuzzi, G. Remuzzi, COVID-19 and Italy: what next? *Lancet* **395**, 1225-1228
422 (2020).
- 423 3. P. Zhou *et al.*, A pneumonia outbreak associated with a new coronavirus of probable bat
424 origin. *Nature* **579**, 270-+ (2020).
- 425 4. N. Zhu *et al.*, A Novel Coronavirus from Patients with Pneumonia in China, 2019. *N.*
426 *Engl. J. Med.* **382**, 727-733 (2020).

- 427 5. S. Flaxman *et al.*, Estimating the effects of non-pharmaceutical interventions on COVID-
428 19 in Europe. *Nature* 10.1038/s41586-020-2405-7, 15.
- 429 6. Y. X. Ng *et al.*, Evaluation of the Effectiveness of Surveillance and Containment
430 Measures for the First 100 Patients with COVID-19 in Singapore - January 2-February
431 29, 2020. *MMWR-Morb. Mortal. Wkly. Rep.* **69**, 307-311 (2020).
- 432 7. R. Pung *et al.*, Investigation of three clusters of COVID-19 in Singapore: implications for
433 surveillance and response measures. *Lancet* **395**, 1039-1046 (2020).
- 434 8. J. R. Koo *et al.*, Interventions to mitigate early spread of SARS-CoV-2 in Singapore: a
435 modelling study. *Lancet Infect. Dis.* **20**, 678–688 (2020).
- 436 9. B. J. Cowling, A. E. Aiello, Public Health Measures to Slow Community Spread of
437 Coronavirus Disease 2019. *J. Infect. Dis.* **221**, 1749-1751 (2020).
- 438 10. B. J. Cowling *et al.*, Impact assessment of non-pharmaceutical interventions against
439 coronavirus disease 2019 and influenza in Hong Kong: an observational study. *Lancet*
440 *Public Health* **5**, E279-E288 (2020).
- 441 11. J. Hellewell *et al.*, Feasibility of controlling COVID-19 outbreaks by isolation of cases and
442 contacts. *Lancet Global Health* **8**, E488-E496 (2020).
- 443 12. J. A. Firth *et al.*, Using a real-world network to model localized COVID-19 control
444 strategies. *Nat. Med.* 10.1038/s41591-020-1036-8.
- 445 13. G. Giordano *et al.*, Modelling the COVID-19 epidemic and implementation of population-
446 wide interventions in Italy. *Nat. Med.* 10.1038/s41591-020-0883-7.
- 447 14. S. Marcel *et al.*, COVID-19 epidemic in Switzerland: on the importance of testing,
448 contact tracing and isolation. *Swiss Medical Weekly* **150** (2020).
- 449 15. S. M. Moghadas *et al.*, The implications of silent transmission for the control of COVID-
450 19 outbreaks. *Proc. Natl. Acad. Sci. U. S. A.* **117**, 17513-17515 (2020).
- 451 16. C. N. Ngonghala *et al.*, Mathematical assessment of the impact of non-pharmaceutical
452 interventions on curtailing the 2019 novel Coronavirus. *Math. Biosci.* **325** (2020).
- 453 17. R. P. Walensky, C. del Rio, From Mitigation to Containment of the COVID-19 Pandemic
454 Putting the SARS-CoV-2 Genie Back in the Bottle. *JAMA-J. Am. Med. Assoc.* **323**, 1889-
455 1890 (2020).
- 456 18. L. Ferretti *et al.*, Quantifying SARS-CoV-2 transmission suggests epidemic control with
457 digital contact tracing. *Science* **368**, 619-+ (2020).
- 458 19. F. Zhou *et al.*, Clinical course and risk factors for mortality of adult inpatients with
459 COVID-19 in Wuhan, China: a retrospective cohort study. *Lancet* **395**, 1054-1062
460 (2020).
- 461 20. J. A. Lewnard *et al.*, Incidence, clinical outcomes, and transmission dynamics of severe
462 coronavirus disease 2019 in California and Washington: prospective cohort study. *BMJ-
463 British Medical Journal* **369**, 10 (2020).
- 464 21. O. Diekmann, J. A. P. Heesterbeek, M. G. Roberts, The construction of next-generation
465 matrices for compartmental epidemic models. *J. R. Soc. Interface* **7**, 873-885 (2010).
- 466 22. B. M. Althouse *et al.*, Stochasticity and heterogeneity in the transmission dynamics of
467 SARS-CoV-2. *arXiv* arXiv:2005.13689, <https://arxiv.org/abs/2005.13689> (2020).
- 468 23. A. Endo, Centre for the Mathematical Modelling of Infectious Diseases COVID-19
469 Working Group, S. Abbott, A. J. Kucharski, S. Funk, Estimating the overdispersion in
470 COVID-19 transmission using outbreak sizes outside China. *Wellcome Open Research*
471 **5**, <https://doi.org/10.12688/wellcomeopenres.15842.12681> (2020).
- 472 24. D. C. Adam *et al.*, Clustering and superspreading potential of SARS-CoV-2 infections in
473 Hong Kong. *Nat. Med.* 10.1038/s41591-020-1092-0, 10.1038/s41591-41020-41092-
474 41590 (2020).
- 475 25. E. S. Rosenberg *et al.*, Cumulative incidence and diagnosis of SARS-CoV-2 infection in
476 New York,. *Ann. Epidemiol.* **48**, 23-29 (2020).

- 477 26. D. B. Larremore *et al.*, Surveillance testing of SARS-CoV-2. *medRxiv*,
478 doi.org/10.1101/2020.1106.1122.20136309 (2020).
- 479 27. A. M. Wilson *et al.*, Quantifying SARS-CoV-2 infection risk within the Apple/Google
480 exposure notification framework to inform quarantine recommendations. *medRxiv*
481 10.1101/2020.07.17.20156539 (2020).
- 482 28. X. He *et al.*, Temporal dynamics in viral shedding and transmissibility of COVID-19. *Nat.*
483 *Med.* **26**, 672-+ (2020).
- 484 29. S. Abbott *et al.*, Estimating the time-varying reproduction number of SARS-CoV-2 using
485 national and subnational case counts [version 1; peer review: awaiting peer review].
486 *Wellcome Open Research* **5**, 112 (2020).
- 487 30. R. Verity *et al.*, Estimates of the severity of coronavirus disease 2019: a model-based
488 analysis. *Lancet Infect. Dis.* **20**, 669-677 (2020).
- 489 31. T. W. Russell *et al.*, Estimating the infection and case fatality ratio for coronavirus
490 disease (COVID-19) using age-adjusted data from the outbreak on the Diamond
491 Princess cruise ship, February 2020. *Eurosurv.* **25**, 12 (2020).
- 492 32. D. C. Buitrago-Garcia *et al.*, Asymptomatic SARS-CoV-2 infections: a living systematic
493 review and meta-analysis. *medRxiv* 10.1101/2020.04.25.20079103 (2020).
- 494 33. M. Cevik *et al.*, SARS-CoV-2, SARS-CoV-1 and MERS-CoV viral load dynamics,
495 duration of viral shedding and infectiousness: a living systematic review and meta-
496 analysis. *medRxiv* 10.1101/2020.07.25.20162107 (2020).
- 497
- 498
- 499

500 **Tables**

501 **Table 1. Parameter values for the model. All rates are in days⁻¹ and many are**
 502 **based on the inverse of measured durations.**

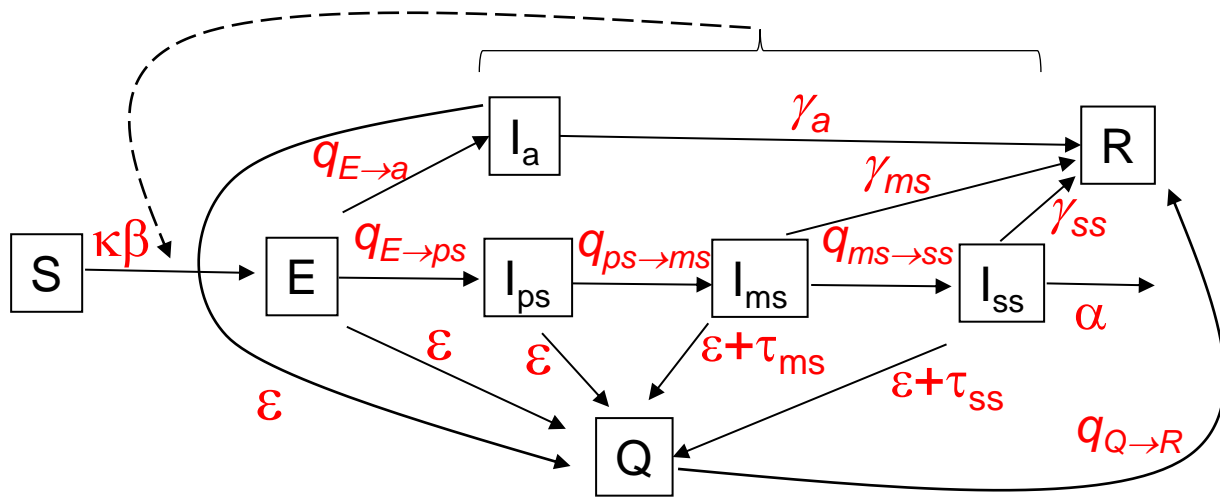
Parameter	Value or range	Description	Reference or Derivation
τ_{ms}	0.2-1	Testing removal rate for I_{ms} (1/delay from onset to testing & tracing)	Scenarios explored
β	0.37	Contact rate	Set to give plausible pre-lockdown $R_0 \cong 2-3$ (29)
f_{tmstr}	0.5 or 1	Fraction of mildly symptomatic cases detected by testing whose contacts were traced	Scenarios explored
κ	0-1	Social distancing factor	Adjusted to produce $R_t \cong 1.2-1.7$; consistent with data post-lockdown; (29)
α	0.0025	Disease caused death rate	estimated from IFR* ($\gamma_{ms} + \gamma_{ss} + q_{E \rightarrow a}$)/(1-IFR) = using infection fatality ratio IFR = 0.0066; (30, 31)
$q_{E \rightarrow a}$	0.078	Transition rate exposed to asymptotically infected	Estimated from $q_{E \rightarrow a} = f_{asymp}(q_{E \rightarrow ps}) / (1 - f_{asymp})$ using fraction asymptomatic ($f_{asymp} = 0.2$); (32)
$q_{E \rightarrow ps}$	1/3.2	1/(duration latent period)	(28)
$q_{ps \rightarrow ms}$	1/2.3	1/(duration pre-symptomatic period)	(28)
$q_{ms \rightarrow ss}$	1/8	1/duration mild symptoms	(19, 20)
γ_a	1/8	Asymptomatic recovery rate	Based on average ratio of shedding durations compared to symptomatic cases (33)
γ_{ms}	1/5,	Mild infection recovery rate	(28)
γ_{ss}	1/10.7	Severe symptom recovery rate	(20)
γ_Q	1/14	Quarantined recover rate	Does not affect dynamics
σ_a	1	Relative infectiousness	(33)

		asymptomatic:mildly symptomatic	
σ_{ps}	1.81	Relative infectiousness pre-symptomatic:mildly symptomatic	(28)
σ_{ms}	1	Relative infectiousness	(reference level)
σ_{ss}	0.008	Relative infectiousness severe symptoms:mildly symptomatic	(28)

503

504

505

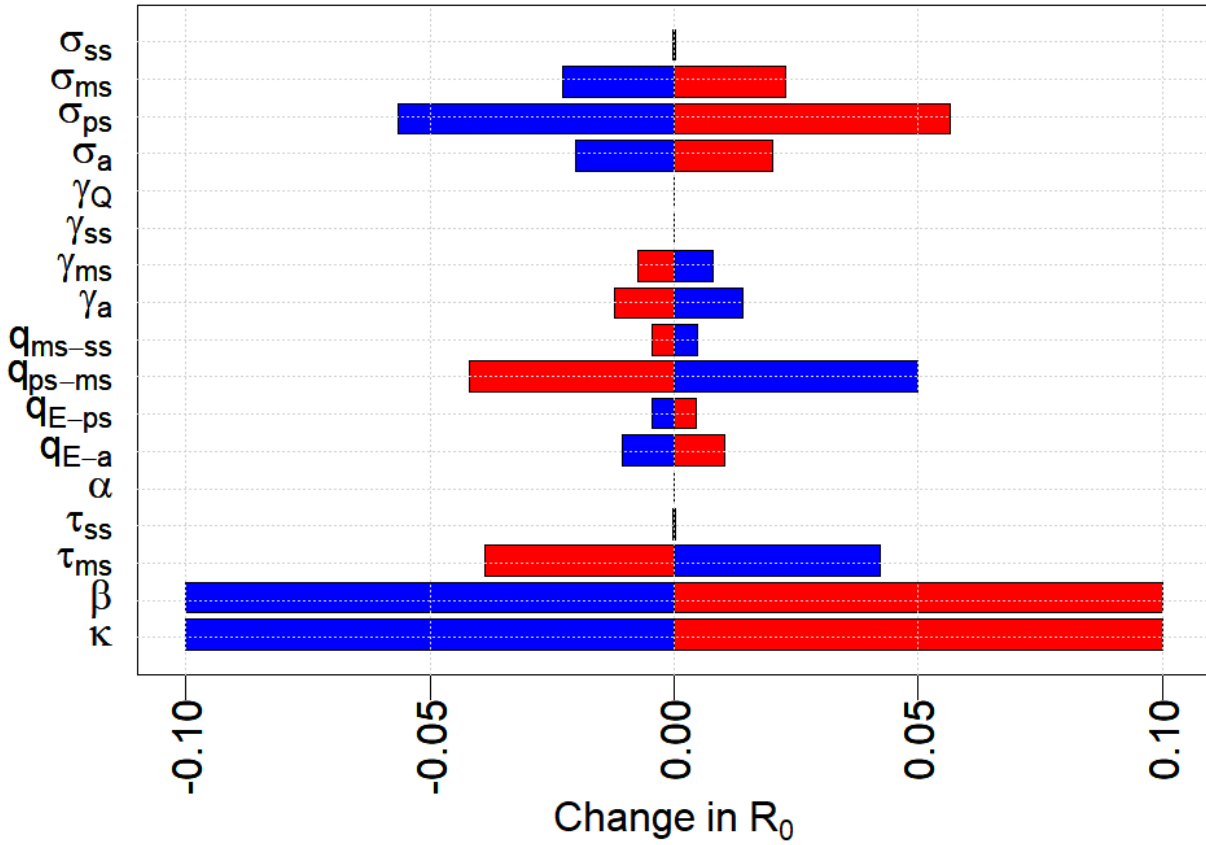


506

507 **Figure S1. Compartmental model of SARS-CoV-2. See text for equations and**
 508 **parameter values. Boxes represent Susceptible (S), Exposed (E), Infected (I),**
 509 **recovered (R), and Quarantined (Q) classes. There are four compartments for**
 510 **infected individuals that reflect symptom severity (asymptomatic, I_a , pre-**
 511 **symptomatic, I_{ps} , mildly symptomatic, I_{ms} , and severely symptomatic, I_{ss}). κ is a**
 512 **social distancing factor between 0 and 1 that modifies the contact rate β , σ are**
 513 **infectiousness for each of the I classes, q are transition rates between classes**
 514 **given by the subscripts separated by the arrow ($q_{E \rightarrow ps}$ is the transition rate**
 515 **between the E and I_{ps} classes), ε is the rate of removal by contact tracing from the**
 516 **E or I classes to the quarantined class Q, τ are the removal rate by testing of**
 517 **mildly symptomatic or severely symptomatic infected individuals, α is the**
 518 **disease-caused death rate, and γ are the recovery rates to the R class. The**
 519 **dashed line and bracket indicate that all 4 classes of infected individuals**
 520 **contribute to transmission.**

521

522



523

524 **Figure S2. Sensitivity analysis. The plot shows how much R_0 changes from a ten**
525 **percent increase (red) or ten percent decrease (blue) in that model parameter**
526 **relative to values in Table 1 (with $\tau_{ms} = 0.2$; $f_{tmstr} = 1$; $\kappa = 1$). R_t scales linearly with β**
527 **and κ , whereas $q_{ps \rightarrow ms}$, τ_{ms} , and σ_{ps} have half as large an effect as β or κ and other**
528 **parameters are even less influential.**

529